## Title
Circulating interleukin-8 levels explain breast cancer osteolysis in mice and humans



## Authors
Kamalakar, Archana
Bendre, Manali S
Washam, Charity L
et al.

## Publication Date
2014-04-01

## DOI
10.1016/j.bone.2014.01.015

Peer reviewed

Published in final edited form as:
*Bone*. 2014 April ; 61: 176–185. doi:10.1016/j.bone.2014.01.015.

# Circulating Interleukin-8 levels explain breast cancer osteolysis in mice and humans

**Archana Kamalakar**[1], **Manali S. Bendre**[1], **Charity L. Washam**[1], **Tristan W. Fowler**[1,2], **Adam Carver**[1], **Joshua D. Dilley**[1], **John W. Bracey**[1], **Nisreen S. Akel**[2], **Aaron G. Margulies**[3], **Robert A. Skinner**[1], **Frances L. Swain**[1], **William R. Hogue**[1], **Corey O. Montgomery**[1], **Parshawn Lahiji**[4], **Jacqueline J. Maher**[4], **Kim E. Leitzel**[5], **Suhail M. Ali**[5], **Alan Lipton**[5], **Richard W. Nicholas**[1], **Dana Gaddy**[1,2], and **Larry J. Suva**[1,2,*]

[1]Department of Orthopaedic Surgery, Center for Orthopaedic Research, Winthrop P. Rockefeller Cancer Institute, University of Arkansas for Medical Sciences, Little Rock, AR

[2]Department of Physiology and Biophysics, University of Arkansas for Medical Sciences, Little Rock, AR

[3]Knoxville Comprehensive Breast Center, Knoxville, TN

[4]Division of Gastroenterology, San Francisco General Hospital, University of California San Francisco Liver Center, San Francisco, CA

[5]Division of Oncology, Pennsylvania State University, Hershey Cancer Institute, Pennsylvania State Hershey Medical Center, Hershey, PA

## Abstract

Skeletal metastases of breast cancer and subsequent osteolysis connote a dramatic change in the prognosis for the patient and significantly increase the morbidity associated with disease. The cytokine Interleukin 8 (IL-8/CXCL8) is able to directly stimulate osteoclastogenesis and bone resorption in mouse models of breast cancer bone metastasis. In this study, we determined whether circulating levels of IL-8 were associated with increased bone resorption and breast cancer bone metastasis in patients, and investigated IL-8 action *in vitro* and *in vivo* in mice. Using breast cancer patient plasma (36 patients), we identified significantly elevated IL-8 levels in bone metastasis patients compared with patients lacking bone metastasis ($p<0.05$), as well as a correlation between plasma IL-8 and increased bone resorption ($p<0.05$), as measured by NTx levels. In a total of 22 ER+ and 15 ER− primary invasive ductal carcinomas, all cases examined stained positive for IL-8 expression. *In vitro*, human MDA-MB-231 and MDA-MET breast cancer cell lines secrete two distinct IL-8 isoforms, both of which were found to stimulate osteoclastogenesis. However, the more osteolytic MDA-MET–derived full length IL-8(1–77) had significantly higher potency than the non-osteolytic MDA-MB-231-derived IL-8(6–77), via the CXCR1 receptor. MDA-MET breast cancer cells were injected into the tibia of nude mice and 7 days later treated daily with a neutralizing IL-8 monoclonal antibody. All tumor-injected mice receiving no antibody developed large osteolytic bone tumors, whereas 83% of the IL-8 antibody-treated mice had no evidence of tumor at the end of 28 days and had significantly increased



Address correspondence to: Larry J. Suva, Ph.D. Center for Orthopaedic Research, Department of Orthopaedic Surgery, University of Arkansas for Medical Sciences, 4301 West Markham St, Little Rock, AR 72205. Phone: (501) 526-6110; Fax: (501) 686-8987; suvalarryj@uams.edu.

survival. The pro-osteoclastogenic activity of IL-8 *in vivo* was confirmed when transgenic mice expressing human IL-8 were examined and found to have a profound osteopenic phenotype, with elevated bone resorption and inherently low bone mass. Collectively, these data suggest that IL-8 plays an important role in breast cancer osteolysis and that anti-IL-8 therapy may be useful in the treatment of the skeletal related events associated with breast cancer.

**Keywords**

Osteoclast; therapy; chemokine; osteolysis

## Introduction

Currently, there are approximately 2 million women in the United States living with breast cancer, and the disease is the second leading cause of cancer death in women [1]. Bone is a common site for cancer metastasis, and bone metastases are frequently associated with complications such as hypercalcemia due to osteolysis, nerve compression, intractable bone pain and pathological fractures [2]. Approximately 80% of women with metastatic breast cancer will have tumors arise in bone during the course of their disease [3].

The diagnosis of distant metastases mandates systemic rather than local primary intervention. Although largely incurable, patient management decisions regarding metastatic breast cancer suggest that initiation of early and aggressive treatment (both local and/or systemic) may be appropriate in some of these patients. The progression of breast cancer bone metastases requires the establishment of functional interactions between metastatic breast cancer cells and bone cells [4]. These interactions are presumably mediated by direct cell-cell contact, and/or soluble stimulators that directly or indirectly induce osteoclast formation and activity [2, 4–6].

In particular, breast cancer metastasis to bone presents unique characteristics which have been successfully targeted in the palliative setting, primarily by the use of bisphosphonates, which target the osteolytic activity of the osteoclast [2, 5, 6] and anti-RANKL therapy [2, 5, 7]. However, targeting the osteoclast alone does little to tumor burden in bone, and suggests that other treatment modalities should be considered.

We and others have shown that the chemokine interleukin 8 (IL-8/CXCL8) is expressed by primary breast cancers and is able to directly stimulate osteoclastogenesis and bone resorption [8–11]. IL-8 is also a potent stimulator of the number and invasiveness of circulating tumor cells (CTCs)especially in tumors with enhanced bone tropism [12–15]. Collectively, these and other data suggest that IL-8 may play an important role in breast cancer progression [16]. One report suggested a correlation of serum IL-8 levels with breast cancer metastasis [17] and recently Singh and colleagues [18] suggested a role for IL-8 in the regulation of patient-derived breast cancer stem-like cell activity. However, the measurement of circulating IL-8 in breast cancer patients with and without bone metastasis and its correlation with levels of bone resorption has not been studied extensively.

Thus, we measured IL-8 in the circulation of breast cancer patients with and without bone metastasis and performed immunocytochemistry on a series of primary human breast cancers, as well as examined IL-8 function *in vivo* and *in vitro*. The data demonstrate that IL-8 is highly expressed by primary human breast cancers and is significantly correlated with elevated bone resorption in breast cancer patients. Tumor-derived systemic IL-8 contributes to increased tumor colonization, tumor growth and bone destruction, and these cellular events can be inhibited by anti-IL-8 therapy.

## Materials and methods

### Reagents

Tissue culture plastics were supplied by Falcon (Lincoln Park, NJ). All other analytical grade reagents were purchased from Sigma (St. Louis, MO) or Fisher (Springfield, NJ). All tissue culture media and reagents were supplied by Life Technologies, Inc. (Grand Island, NY). Recombinant human RANKL, recombinant murine macrophage colony stimulating factor (CSF-1), recombinant human IL-8, IL-8(1–77), IL-8(6–77) and control IgG were purchased from R&D Systems (Minneapolis, MN). Anti-IL-8 antibodies used *in vivo* were obtained from R&D Systems.

### Patient Samples

Archival breast cancer patient plasma was obtained from 36 patients (18 with and 18 without bone metastasis) for the measurement of IL-8. Analysis of the archival plasma samples was approved by the University of Arkansas for Medical Sciences and Pennsylvania State University Institutional Review Boards. The clinical assessment of bone metastasis was based on patient bone scan, x-ray evidence of bone metastasis, and elevated blood N-Telopeptide (NTx) levels, a clinical marker of bone resorption [19]. The serum NTx levels of all patients were used to help discern the presence or absence of bone metastasis. The women ranged in age from 49–92 years with a median age of 70 in the ‘bone metastasis’ group and 67 in the ‘no bone metastasis’ group. A power analysis was conducted to confirm that the size of the sample was sufficient to provide a statistical power of more than 80%.

In addition, a series of archival formalin-fixed paraffin embedded tumor tissue samples from 22 ER+ (expressing 2+ − 3+ positivity in > 50% cells) and 15 ER- invasive ductal breast carcinomas, irrespective of grade and stage of disease, were also selected for evaluation. Unstained sections were immunostained for IL-8 expression (anti-IL-8 antibody, dilution 1:200, R&D Systems, Minneapolis, MN) with appropriate positive and negative controls. The intensity of staining for IL-8 was graded on a scale of 0 to 3+ with 0 representing no detectable staining and 3+ representing the strongest staining. Two independent observers examined each slide.

### Cell Lines and Culture Conditions

The MDA-MB-231 cells (MDA-231), MDA-MET cell lines and transfected variants (sense and anti-sense) were maintained in DMEM, supplemented with 10% fetal bovine serum at 37°C in sterile culture dishes [9]. Highly bone metastatic MDA-MET cells were derived from a weakly osteolytic MDA-231 variant by *in vivo* selection [9]. MDA-MET cells secrete full length IL-8 and produce osteolytic lesions (100%) within 4 weeks of inoculation in the circulation or tibia of athymic nude mice [20] and grow effectively in the mammary fat pad [21] compared with MDA-231 cells that produce little full-length IL-8 [20].

MDA-231-IL8 and MDA-MET-AS cells were generated by stable transfection of expression vectors (pcDNA3 Invitrogen, Carlsbad, California) expressing full length hIL-8 or anti-sense hIL-8 cDNA as a *HindIII–BamHI* fragment by calcium phosphate precipitation. The pcDNA3/IL-8 sense or antisense (AS) DNA transfected cells were grown and single clones isolated by limiting dilution in the presence of the selective marker, G418 (Sigma Chemical Co., St. Louis, Missouri, USA). Clones were screened by measuring the amount of secreted hIL-8 (in sense expressing MDA-231 or the loss of IL-8 in MDA-MET antisense cells) in serum-free 48-h conditioned media. Clones with significantly increased and decreased IL-8 levels respectively were selected for further study.

HEK-293 human embryonal kidney cells stably expressing CXCR1 or CXCR2 (a generous gift from Dr. Ji Ming Wang, NCI Frederick Cancer Research) were grown as monolayers in growth medium (Dulbecco's modified Eagle's medium with 10% fetal calf serum, penicillin (100 units/ml), and streptomycin (100 μg/ml)). Cells were grown to approximately 75% confluency in an atmosphere of 95% air, 5% CO2at 37°C as described [22].

### IL-8 ligand binding assay

Ligand binding assays were performed as described [23]. Briefly, duplicate aliquots of stably transfected CXCR1 or CXCR2 HEK-293 cells (5×105–1×106 cells/200ul) were re-suspended in binding medium (RPMI 1640. 10 mg/ml BSA; 25 mM HEPES; 0.05% Na azide) in the presence of 0.1 ng $^{125}$IL-8 (DuPont-NEN, DE) and serial dilutions of unlabeled IL-8(1–77 or 6–77). Following 1h incubation at room temperature the cells were centrifuged through 0.8ml sucrose in PBS and the radioactivity remaining in the cell pellets was measured in a 1272 CliniGamma gamma counter (Pharmacia, MD).

### Intratibial injection of tumor cells, antibody treatment and survival

MDA-MET, MDA-231-IL8 and MDA-MET-AS cells were grown to sub-confluence. Fresh medium was added 24 hours before harvesting for tumor inoculation. On the day of the injections, cells were harvested with 0.2% EDTA and 0.02% trypsin, washed twice in PBS and resuspended in PBS at a concentration of $10^6$ cells/ml. Four-week-old athymic female nude mice were used for all tumor inoculations, were purchased from Taconic Farms (Taconic, NY) and housed in an approved animal facility with protocols approved by the University of Arkansas for Medical Sciences Institutional Animal Care and Use Committee.

Before injection, the animals were deeply anesthetized with a 1:1:4.6 solution of xylazine:ketamine:PBS (administered i.p. at 0.033-ml mixture/10-g body weight) as described [20]. The mice were placed in a prone position and after gently palpating the tibia, the upper end of the tibia was identified as the site for injection. Approximately 10,000 cells (in 10μl) were injected into the right tibia of nude mice using a 50μl syringe and 28 gauge needle. PBS only was injected in the left leg as vehicle control. After injection, the mice were placed on a heating pad to recover from anesthesia and then returned to their cages.

For the experiments using antibody treatments, animals were randomized into 3 groups: IL-8 antibody group (20 mice), Control IgG antibody group (20 mice) and no antibody group (15 mice). The IL-8 antibody (~35μg/animal) group or control antibody group (~35μg/animal) were injected intraperitoneally every alternate day in the animals from the respective groups, starting 7 days after the intratibial injections of MDA-MET cells and continuing for 4 weeks. Animals in the no antibody group did not receive either antiserum and were injected only with PBS.

All mice were followed for periods of up to 4 weeks, then sacrificed and X-rayed (Kodak X-Omat, Rochester, NY) as described below. Dissected legs were processed for histopathology. Tumor growth in bone was monitored by weekly X-ray of deeply anesthetized nude mice using an AXR minishot 110 X-ray cabinet (Associated X-ray corporation, East Haven, CT) at 3 mA, 33 kV for 20 s using Kodak X-Omat TL film (Kodak, Rochester, NY) and processed on a Kodak X-Omat RP automated film processor.

All tumor-bearing and contralateral legs were excised, fixed in 10% neutral-buffered formalin for 2 days. The specimens were then imaged in formalin by micro computed tomography (MicroCT).

Another series of MDA-MET tumor-bearing animals including an IL-8 antibody group (30 mice) and a control IgG-treated antibody group (30 mice) were followed specifically for

survival. Survival was defined as time to moribund state or hind limb paralysis, at which point mice were sacrificed. Antibody treatment began on day 5 after tumor inoculation. Analysis of survival endpoints was blinded. All deaths were recorded throughout the time course of the anti-IL-8 antibody and control IgG injections (injections were halted at after 28 days of antibody injection), corresponding to day 33 following tumor inoculation. All remaining mice were sacrificed and femurs/tibias harvested.

### Human IL-8 transgenic mice

The generation of mice with a liver-specific transgene encoding human IL-8 has been described previously [24]. These mice have circulating neutrophilia and impaired chemotaxis to intraperitoneal thioglycollate, but organ histology and function have been reported as normal [25], with no description of a bone phenotype. Genotype was confirmed by the measurement of human IL-8 in mouse serum. IL-8 levels in transgenic mice (hIL-8 Tg) averaged 70 ng/ml, and were undetectable in WT mice.

### Bone Phenotyping

All micro computed tomography (MicroCT) analyses were consistent with current guidelines for the assessment of bone microstructure in rodents using MicroCT [26]. Formalin-fixed tibiae and femora from tumor bearing mice and controls, as well as from IL-8 transgenic mice were imaged using a MicroCT 40 (Scanco Medical AG, Bassersdorf, Switzerland) using a 12 μm isotropic voxel size in all dimensions as described previously [27]. Three-dimensional reconstructions were created by stacking the regions of interest from each two-dimensional slice and then applying a gray-scale threshold and Gaussian noise filter as described [27] using a consistent and predetermined threshold (245) with all data acquired at 55 kVp, 114 mA, and 200-ms integration time. Fractional bone volume (bone volume/tissue volume; BV/TV) and architectural properties of trabecular bone (trabecular thickness (Tb.Th.; μm), trabecular number (Tb.N.; mm −1), and connectivity density (Conn. D.; $mm^3$) were calculated using previously published methods [28]. In addition, for cortical bone analysis of IL-8 transgenic mice, MicroCT slices were segmented into bone and marrow regions by applying a visually chosen, fixed threshold for all samples after smoothing the image with a three-dimensional Gaussian low-pass filter ($\sigma = 0.8$, support = 1.0) to remove noise, and a fixed threshold (245). Femoral cortical geometry was assessed in a 1-mm-long region centered at the femoral midshaft. The outer contour of the bone was found automatically using the built-in manufacturer's contouring tool. Total area was calculated by counting all voxels within the contour, bone area by counting all voxels that were segmented as bone, and marrow area was calculated as total area - bone area. This calculation was performed on all 25 slices (1 slice = ~12.5 μm), using the average for the final calculation. The outer and inner perimeter of the cortical midshaft was determined by a three-dimensional triangulation of the bone surface (BS) of the 25 slices, and cortical thickness and other cortical parameters were determined as described [27, 28]. For bone phenotype assessment of IL-8 transgenic mice, 10 male and 6 female IL-8 transgenic mice (4 months) and 9 male and 6 female WT littermate controls were examined. Serum IL-8 levels were measured to determine the genotype of the mice [25], and blood was drawn and serum prepared for serum bone biochemical marker analyses.

Where necessary, mechanical testing of femurs was performed as described previosly [28]. Briefly, specimens were tested at room temperature using a servohydraulic-testing machine MTS 858 Bionex Test Systems load frame (MTS, Eden Prairie, MN) with computer control, data logging, and calculations of load to failure using TestWorks version 4.0 (MTS). Bones were placed with their anterior side down on two horizontal supports spaced 7 mm apart; the central loading point contacted the posterior surface of the diaphysis at the midpoint of the bone length. The loading point was displaced downward (transverse to the long axis of the

bone) at 0.1 mm/s until failure, generating bending in the anterior-posterior plane. Load-displacement data were recorded at 100 Hz (TestWorks 4.0, MTS) and test curves were analyzed to determine measures of whole-bone strength, primarily peak load and stiffness as we have described [28]. Load to failure was recorded as the load after a 2% drop from peak load.

### Histology and Histomorphometry

Following MicroCT imaging, the specimens were decalcified in 5% formic acid with agitation until deemed clear by the ammonium oxalate endpoint test [9]. The decalcified specimens were then dehydrated through graded ethanol, cleared in methyl salicylate, embedded in paraffin, sectioned (5 um) and stained with hematoxylin and eosin (H&E) and tartrate resistant acid phosphatase (TRAP) as described [28, 29]. In each section, 10 fields were counted at 40× magnification, starting one field below the growth plate and proceeding from the cortical surface on one side to the cortical surface to the other. The histomorphometric parameters measured included total area, total bone area, tumor area, bone perimeter, eroded perimeter and osteoclast number as described previously [9].

### Bone resorption and human IL-8 Assays

Serum was collected from all animals at the time of sacrifice and was stored at −80°C. Serum was thawed and the assay performed according to the individual manufacturer's instructions. A RatLaps ELISA (Immunodiagnostic Systems Inc, Scottsdale, AZ) was used as a quantitative assay for the determination of bone-related degradation products from C-terminal telopeptides of type I collagen in mouse serum. Human IL-8 was measured using a commercially available assay (Alpco, Salem, NH).

### Osteoclastogenesis

Peripheral blood mononuclear cells (PBMCs) were purchased (Astarte Biologics, Redmond, WA) and cultured towards osteoclast development as described previously [10]. Briefly, cells were counted with a hemocytometer and plated in 96 well tissue culture plates at a concentration of 0.25 million cells in 250μL volume per well. Macrophage colony stimulating factor (CSF-1; 25 ng/ml) was added to all groups. IL-8(1–77) and IL-8(6–77) were tested and different concentrations and RANKL (25 ng/ml) was used as a positive control. Cultures were maintained at 37°C and half-feeds performed three times per week, and terminated on the $10^{th}$ day. Medium was aspirated and the cells fixed with 10% formalin. TRAP staining was performed (Sigma, St Louis, MO) for quantification of TRAP + multinucleated cells (MNCs). TRAP+ cells having more than 3 nuclei were counted as osteoclasts, and osteoclast cell counts in each well were averaged and the results expressed as the number of TRAP+ MNCs/well per treatment group (n = 4 wells per treatment) [10].

### Statistical analysis

Data were analyzed by analysis of variance (ANOVA) with Bonferroni's post-test or by Student's t-test as appropriate. All data are presented as mean ± SEM. $p<0.05$ between groups was considered significant and is reported as such. Survival curves were created using SigmaStat 2.03 (Systat Software Inc, San Jose, CA). The log-rank test (Wilcox survival) was used to analyze survival data. $p<0.05$ between the two treatment groups was considered significant and is reported as such.

## Results

### IL-8 is expressed by primary human breast tumors

To determine whether IL-8 was expressed in primary human breast tumors archival tumor tissue samples from 22 ER+ and 15 ER− invasive ductal breast carcinomas were selected for this study under an Institutional IRB-approved protocol. The tumors were immunostained and IL-8 staining intensity graded on a scale of 0 to 3+, with 0 representing no detectable staining and 3+ representing the strongest staining (Figure 1). 100% of cases examined stained positive for IL-8 expression. 68% of ER+ cases showed 3+ IL-8 staining compared with 47% of ER-cases (Table 1). No significant difference was observed in the intensity of IL-8 staining between ER+ and ER− cases. IL-8 expression was common in invasive ductal breast carcinomas and the level of IL-8 expression did not correlate with ER status, indicating that in these samples, IL-8 expression in primary breast cancer is independent of ER status.

### Circulating IL-8 is correlated with bone resorption in breast cancer patients

Since the expression of IL-8 was common in primary human breast cancer, we next examined circulating IL-8 levels in the plasma of breast cancer patients with and without clinical evidence of bone metastasis [30]. Plasma IL-8 levels were significantly elevated in breast cancer patients with bone metastasis (mean 4.4 ± 1.8 pg/ml) compared with breast cancer patients with no bone metastasis (mean 2.1 ± 0.9 pg/ml) (Figure 2A). Since these patients also had known serum NTx values [30] (a circulating measure of bone resorption) we also determined if plasma IL-8 was correlated with serum NTx (Figure 2B). Indeed, there was a significant positive correlation between serum NTx and plasma IL-8 levels (r=0.7279). These data demonstrate that IL-8 is expressed by primary breast tumors, circulates at higher levels in breast cancer patients with bone metastasis, and is significantly correlated with bone resorption.

### Tumor-derived IL-8 peptides stimulate osteoclastogenesis

MDA-MET cells form large tumor foci with extensive bone destruction when injected directly into the tibia of nude mice, whereas MDA-MB-231 cells do not [20]. In addition, the more osteolytic MDA-MET tumors cells secrete high levels of full length IL-8(1–77) [20], whereas the less osteolytic MDA-MB-231 cells secrete a truncated (6–77) IL-8 isoform [20]. In order to determine the biological activity of these specific IL-8 isoforms, the ligand binding affinity of the peptides for the human IL-8 receptors (CXCR1 and CXCR2) was determined using HEK-293 cells, stably expressing the receptors (Figure 3A, B) [22]. In addition, the capacity of both human IL-8 peptides to stimulate osteoclastogenesis was determined in cultures of human peripheral blood mononuclear cells (Figure 3C). IL-8 ligand affinity binding studies demonstrated a higher affinity of IL-8(1–77) (IC50 ~$5\times10^{-9}$M) than IL-8(6–77) (IC50 ~$10^{-6}$M) for CXCR1, but similar affinities for CXCR2 (Figure 3A, B). Next, we observed that full-length IL-8(1–77) significantly stimulated human osteoclast formation at 10 and 100nM as did IL-8(6–77), albeit to a significantly lesser extent than IL-8(1–77) (Figure 3C). These data suggest that human osteoclastogenesis can be induced by both IL-8 peptides, but that the activity of the full length 1–77 peptide is greater than the truncated 6–77 peptide. Interestingly, the pro-osteoclastogenic effect of IL-8 on human osteoclasts was dose-dependently inhibited by Repertaxin, a small molecule inhibitor of CXCR1 and 2 [31] (Figure 3D), with no effect on RANKL-induced osteoclastogenesis, demonstrating the direct action of IL-8 on CXCR1 expressed on osteoclasts and their precursors [10].

### Anti-IL-8 antibody inhibits tumor osteolysis and improves survival

Three groups of MDA-MET tumor-bearing mice were treated with either a monoclonal antibody directed against IL-8 (35 μg/mouse), or an isotype control IgG (35 μg/mouse), or no treatment every alternate day for 4 weeks beginning 7 days after direct tumor cell inoculation into the tibia. All animals receiving no treatment (15/15) or treated with control IgG (20/20) developed large osteolytic bone tumors (Figure 4A). No differences in tumor burden or any other tumor parameter were observed between the untreated or IgG treated control groups. In contrast, in the IL-8 antibody treated group 15/20 animals had no histological evidence of tumor. Small tumor foci with no measureable osteolysis were observed in 3 mice and 2 animals developed small osteolytic tumors (Figure 4A).

The IL-8 antibody treated group had smaller tumors and more bone remaining than either the IgG-treated or no antibody groups (Figure 4B–D). Both the total area of osteolysis as well as tumor burden was significantly lower in mice treated with IL-8 antibody compared with mice receiving control IgG or no treatment. The higher bone area remaining in the IL-8 antibody group compared with the IgG-treated or no antibody group was due to decreased number of osteoclasts (Figure 4C) and decreased eroded bone surface (data not shown). In sum, IL-8 antibody treatment significantly decreased tumor development, osteoclast formation and the resultant bone destruction (Figure 4).

Next, the serum bone resorption marker NTx was measured by ELISA in IL-8 antibody and IgG-treated tumor-bearing mice, as well as non-tumor bearing controls. Bone resorption in non-treated tumor bearing mice was significantly increased compared to both IL-8 antibody treated and non-tumor bearing mice (Figure 4E). Animals treated with IL-8 antibody had levels of bone resorption not different from nontumor bearing animals (Figure 4E), indicating that the IL-8 antibody decreased all the bone resorption associated with the presence of tumor. Since the level of bone resorption in the IL-8 antibody treated group was not significantly different from the bone resorption in non-tumor bearing mice, it suggests that tumor-derived IL-8 was entirely responsible for the elevated bone resorption (Figure 4E). Importantly, survival of tumor-bearing mice treated with IL-8 antibody was significantly improved (Figure 4F).

### IL-8 expression alters the osteolytic phenotype of breast cancer cells

To evaluate the effect of IL-8 expression on the phenotype of MDA-231 tumor cells *in vivo*, we engineered a series of MDA-231-derived cell lines which stably expressed either hIL-8 cDNA (MDA-231-IL8) or hIL-8 antisense cDNA (MDA-MET-AS). Increased expression or knockdown of IL-8 was confirmed by IL-8 ELISA (Figure 5).

All animals injected with MDA-231-IL8 cells secreted high levels of IL-8 compared with MDA-231 cells (Figure 5A) and produced large tumors with clear evidence of extensive osteolysis (Figure 5B). Histomorphometric analysis revealed that the animals injected with MDA-231-IL8 cells had less remaining bone due to increased numbers of osteoclasts (Supplemental Figure 1A, B). No effects on cell proliferation were observed in MDA-231-IL8 cells *in vitro* (Supplemental Figure 2A). Thus, the increased IL-8 secretion due to transfection of MDA-231 cells with IL-8 cDNA enhanced both osteoclast formation and bone destruction.

In the animals injected with the MDA-MET-AS cells, ~80% had evidence of tumor histologically and the tumor foci were much smaller than in any of the control MDA-MET injected animals, with few MDA-MET-AS animals (20%) having evidence of osteolysis (Figure 5D). The osteolysis appeared to be associated with the diminished levels of IL- 8 expression by MDA-MET-AS cells (Figure 5C). The reduction in IL-8 secretion in MDA-

MET-AS cells significantly decreased tumor burden and osteoclast formation (Supplemental Figure 1C, D) as well as bone destruction *in vivo* (Figure 5D), but had no effect on tumor cell proliferation *in vitro* (Supplemental Figure 2B). The modulation of IL-8 secretion by human breast cancer cells significantly and selectively altered osteoclastogenesis and bone resorption *in vivo*.

### Skeletal phenotype of human IL-8 transgenic mice

Since we have shown that MDA-MET cells secrete a variety of osteoclastogenic factors in addition to IL-8 [10, 20], we next evaluated the bone phenotype of transgenic mice expressing human IL-8 [24] to confirm that IL-8 overexpression *in vivo* was indeed responsible for the profound osteolytic phenotype.

Gross changes in tibial and femoral morphology or bone length of WT or hIL-8 Tg mice were not apparent (data not shown). However, a significant decrease in the fractional bone volume (BV/TV) of both the femur and tibia of hIL-8 Tg mice was observed (Figure 6A, B). In addition, and entirely consistent with the dramatic decrease in BV/TV, trabecular number (Tb.N.) was significantly decreased, coupled with significantly increased trabecular separation (Tb.Sp) with no significant difference in trabecular thickness (Tb.Th.) in hIL-8 Tg mice (Figure 6C–E). The low bone mass phenotype was evident in mice as young as 2 months (the earliest age examined) and was evident in both genders (data not shown). The MicroCT data analysis presented (Figure 6) was obtained from adult mice at 4 months of age.

In addition to the trabecular microarchitecture, the cortical bone geometry of hIL-8 Tg mice was examined by MicroCT in the mid-diaphysis of the femur (Figure 7). The cortical thickness of the femur was significantly decreased in hIL-8 Tg mice (Figure 7), and medullary area of the femur significantly increased by the transgenic expression of hIL-8 (Figure 7C). As expected, the changes in cortical geometry were reflected in the significantly decreased peak load-to-failure of femurs from hIL-8 Tg mice, compared with WT control femurs in 3 point bending tests (Figure 7D) [28].

Consistent with the MicroCT evaluation, histomorphometric analysis of the long bones confirmed the decreased bone volume (data not shown) and indicated that this effect was associated mechanistically with a significant increase in the number of osteoclasts, as measured by the number of osteoclasts per bone perimeter (NOc/BPm) (Figure 8A, B). In addition and consistent with the histomorphometry and the MicroCT analysis, serum measures of NTx, an *in vivo* biomarker of osteoclast activity, revealed a significant increase in bone resorption in hIL-8 Tg mice compared with WT (Figure 8C). No changes in any osteoblast parameters were observed (data not shown) but there was a striking and significant increase in marrow adiposity (Figure 8D, E). Collectively, these data suggest that the decreased bone mass in hIL-8 Tg mice is the result of increased osteoclast number and activity, that is associated with an increase in marrow fat (Figure 8D, E) and no demonstrable change in osteoblast parameters driven by transgenic IL-8 expression.

## Discussion

IL-8 is expressed by a number of cancer cell lines *in vitro*. A correlation has been observed between tumor cell expression of IL-8 and metastatic potential in a variety of cancer settings [8, 9, 32–37]. In addition, serum levels of IL-8 are increased in patients with breast cancer and appear to be an independent prognostic indicator for post-relapse survival [17, 38], with similar results reported for prostate cancer [39] and squamous cell carcinoma patients [40]. Others have shown that breast cancer cells can induce the release of lysophosphatidic acid (LPA) from activated platelets which, in turn, promotes tumor cell proliferation and the

LPA-dependent secretion of IL-6 and IL-8, thereby enhancing tumor growth and osteolysis [41]. Collectively, these data suggest that IL-8 expression is an important mediator of osteoclastogenesis and bone destruction, once breast cancer cells are seeded in the bone microenvironment [42].

Our data demonstrate that primary human invasive ductal carcinomas express IL-8 and that the level of expression does not appear to correlate with ER status. These observations in primary human breast cancers are contrary to previously published *in vitro* observations which have shown IL-8 expression was shown to be significantly correlated with ER status [43]. Our study also highlights the importance of measuring circulating IL-8 and demonstrates that tumor osteolysis and circulating plasma IL-8 levels are significantly positively correlated. In light of previous observations demonstrating the important role of IL-8 in breast cancer growth, invasion and metastasis [18, 42], further investigation is warranted to determine if IL-8 is an independent prognostic indicator in breast cancer.

We have shown that osteolytic MDA-MET cells secrete full-length IL-8, whereas non-osteolytic MDA-MB-231 cells secrete a truncated (6–77) form of the protein [20]. Similar IL-8 isoform expression has also been reported in ovarian cancer [44]. In the current study, the distinct osteoclastogenic activities of the secreted isoforms of IL-8 and their specific CXCR1 binding affinities correlate with osteoclastogenic activity. We propose that the MDA-MET breast cancer growth advantage in bone compared with MDA-MB-231 [21] is not due to a simple proliferative advantage, but to the ability of MDA-MET to profoundly stimulate osteoclastic bone resorption [10], via the secretion of full-length IL-8. *In vivo*, it appears that the increased osteolysis of MDA-MET cells is entirely attributable to increased IL-8 secretion, since inhibition of IL-8 activity in MDA-MET tumor bearing mice reduces bone resorption to that found in serum of non-tumor bearing mice. This idea is further supported by the altered phenotype *in vivo* of breast cancer cells engineered for increased or decreased expression of IL-8 and by the severely osteopenic bone phenotype of hIL-8 Tg mice. In all, these functional data are entirely consistent with our earlier demonstration that MDA-MET conditioned medium (containing IL-8(1–77) stimulates human osteoclast formation more than MDA-231 conditioned medium containing IL-8(6–77) and that CXCR1 and not CXCR2 is expressed in human osteoclasts and their precursors [10, 20]. The investigation of the activity of these two IL-8 isoforms *in vitro* and *in vivo* is ongoing and promises to provide new insight into the role of IL-8 in breast cancer progression in bone.

Different amino terminal variants of endogenous IL-8 with similar relative stability have been described previously [45], with IL-8(1–77) and IL-8(6–77) the major forms derived from endothelial cells or fibroblasts and leukocytes [46, 47]. We and others have previously reported tumor-specific isoforms [20, 44]. In ligand binding assays in other cell types, some shorter forms of IL-8 have been demonstrated to have slightly higher affinity than IL-8(1–77) [46], provided the Glu-Leu-Arg (ELR) motif (found at position 9–11) remains intact [46]. Although differing affinities have been reported for these shorter IL-8 isoforms, our study is the first to report the altered activity of two IL-8 isoforms on osteoclast formation, demonstrating that full length IL-8(1–77) has more potent osteoclastogenic effects than IL-8(6–77).

Although we and others have shown that tumor-derived IL-8 induces murine osteoclastogenesis and bone resorption *in vivo*, these observations could be explained by the requirement for other tumor-derived activity(s). Hence, we sought to clearly demonstrate that IL-8 was able to induce osteoclast formation in the mouse *in vivo* in the absence of tumor, using IL-8 transgenic mice, rather than resolve the IL-8 pharmacokinetic and pharmacodynamic issues that plague the injection of protein agents into mice.

IL-8 transgenic mice are perfectly viable and were first reported in 1994 [24]. The mice have been shown to have impaired neutrophil migration, but no skeletal phenotype has been reported. The mice express full length human IL-8(1–77) selectively in the liver via the human apoE promoter and its liver-specific enhancer (HCR) [24]. It should be noted that mice do not normally express IL-8, but do express an ortholog of the specific IL-8 receptor CXCR1 and are exquisitely sensitive to human IL-8 [24, 25].

MicroCT analysis revealed a dramatic decrease in BV/TV as well as micro-architectural parameters of trabecular bone, consistent with severe osteopenia due to markedly increased osteoclastic activity. The osteopenia was also observed in the cortical compartment. IL-8 Tg mice had significant decreases in cortical bone geometry leading to decreased load to failure (and bone strength). Similarly, histomorphometry and serum measurement of the bone resorption marker NTx demonstrated a significant increase in bone resorption in IL-8 Tg mice compared with litter mate controls. In support of this notion, TRAP staining of osteoclasts on the bone surface demonstrated increased numbers of osteoclasts. These data directly support our hypothesis that IL-8 is a potent osteoclastogenic agent and that IL-8, independent of other tumor-derived factors, is able to stimulate the induction of osteoclastogenesis and bone resorption.

Tumor growth in bone depends on a number of factors, including osteoclastogenesis, bone resorption, and angiogenesis, as well as cell-cell interactions [5]. Osteolytic tumor cells accomplish this by secreting factors that increase the number of mature osteoclasts and the activity of individual osteoclasts and that support angiogenesis, such as IL-8. An understanding at the molecular level of the mechanisms supporting and stimulating tumor osteolysis, and regulating survival, may provide important insight into more effective therapies for this devastating complication of cancer, including ones that target multifunctional molecules such as specific IL-8 isoforms.

## Supplementary Material

Refer to Web version on PubMed Central for supplementary material.

## Acknowledgments

This work was supported by NIH R01 CA166060-01A1 (LJS), a Pilot grant from AR Breast Cancer Research Program (ABCRP) (LJS), the Carl L. Nelson Chair of Orthopaedic Creativity (LJS), a Graduate Studentship from the ABCRP (CLW), and the UAMS Translational Research Institute (TRI) (CTSA grant Award #1 UL1TR000039) and is dedicated to the memory of the late Dr. Carl L. Nelson.

## References

1. Coleman RE. Adjuvant bisphosphonates in breast cancer: are we witnessing the emergence of a new therapeutic strategy? Eur J Cancer. 2009; 45:1909–1915. [PubMed: 19447606]
2. Mundy GR. Metastasis to bone: causes, consequences and therapeutic opportunities. Nat Rev Cancer. 2002; 2:584–593. [PubMed: 12154351]
3. Suva LJ. Adjuvant bisphosphonates in breast cancer: the ABCSG-12 study. Curr Osteoporos Rep. 2010; 8:57–59. [PubMed: 20425611]
4. Suva LJ, Griffin RJ, Makhoul I. Mechanisms of bone metastases of breast cancer. Endocr Relat Cancer. 2009; 16:703–713. [PubMed: 19443538]
5. Suva LJ, Washam C, Nicholas RW, Griffin RJ. Bone metastasis: mechanisms and therapeutic opportunities. Nat Rev Endocrinol. 2011; 7:208–218. [PubMed: 21200394]
6. Weilbaecher KN, Guise TA, McCauley LK. Cancer to bone: a fatal attraction. Nat Rev Cancer. 2011; 11:411–425. [PubMed: 21593787]

7. Roodman GD. Mechanisms of bone metastasis. N Engl J Med. 2004; 350:1655–1664. [PubMed: 15084698]
8. De Larco J, Wuertz B, Rosner K, Erickson S, Gamache D, Furcht L. A potential role for interleukin 8 in the metastatic phenotype of breast carcinoma cells. American Journal of Pathology. 2001; 158:639–646. [PubMed: 11159200]
9. Bendre MS, Gaddy-Kurten D, Mon-Foote T, Akel NS, Skinner RA, Nicholas RW, Suva LJ. Expression of Interleukin 8 and not Parathyroid Hormone-related Protein by Human Breast Cancer Cells Correlates with Bone Metastasis in Vivo. Cancer Res. 2002; 62:5571–5579. [PubMed: 12359770]
10. Bendre MS, Montague DC, Peery T, Akel NS, Gaddy D, Suva LJ. Interleukin-8 stimulation of osteoclastogenesis and bone resorption is a mechanism for the increased osteolysis of metastatic bone disease. Bone. 2003; 33:28–37. [PubMed: 12919697]
11. Lu Y, Cai Z, Xiao G, Keller ET, Mizokami A, Yao Z, Roodman GD, Zhang J. Monocyte chemotactic protein-1 mediates prostate cancer-induced bone resorption. Cancer Res. 2007; 67:3646–3653. [PubMed: 17440076]
12. Charafe-Jauffret E, Ginestier C, Iovino F, Wicinski J, Cervera N, Finetti P, Hur MH, Diebel ME, Monville F, Dutcher J, Brown M, Viens P, Xerri L, Bertucci F, Stassi G, Dontu G, Birnbaum D, Wicha MS. Breast cancer cell lines contain functional cancer stem cells with metastatic capacity and a distinct molecular signature. Cancer Res. 2009; 69:1302–1313. [PubMed: 19190339]
13. Kim MY, Oskarsson T, Acharyya S, Nguyen DX, Zhang XH, Norton L, Massague J. Tumor self-seeding by circulating cancer cells. Cell. 2009; 139:1315–1326. [PubMed: 20064377]
14. Ginestier C, Liu S, Diebel ME, Korkaya H, Luo M, Brown M, Wicinski J, Cabaud O, Charafe-Jauffret E, Birnbaum D, Guan JL, Dontu G, Wicha MS. CXCR1 blockade selectively targets human breast cancer stem cells in vitro and in xenografts. J Clin Invest. 2010; 120:485–497. [PubMed: 20051626]
15. Fernando RI, Castillo MD, Litzinger M, Hamilton DH, Palena C. IL-8 signaling plays a critical role in the epithelial-mesenchymal transition of human carcinoma cells. Cancer Res. 2011; 71:5296–5306. [PubMed: 21653678]
16. Korkaya H, Wicha MS. Breast cancer stem cells: we've got them surrounded. Clin Cancer Res. 2013; 19:511–513. [PubMed: 23251003]
17. Benoy IH, Salgado R, Van Dam P, Geboers K, Van Marck E, Scharpe S, Vermeulen PB, Dirix LY. Increased serum interleukin-8 in patients with early and metastatic breast cancer correlates with early dissemination and survival. Clin Cancer Res. 2004; 10:7157–7162. [PubMed: 15534087]
18. Singh JK, Farnie G, Bundred NJ, Simoes BM, Shergill A, Landberg G, Howell SJ, Clarke RB. Targeting CXCR1/2 significantly reduces breast cancer stem cell activity and increases the efficacy of inhibiting HER2 via HER2-dependent and -independent mechanisms. Clin Cancer Res. 2013; 19:643–656. [PubMed: 23149820]
19. Glover SJ, Gall M, Schoenborn-Kellenberger O, Wagener M, Garnero P, Boonen S, Cauley JA, Black DM, Delmas PD, Eastell R. Establishing a reference interval for bone turnover markers in 637 healthy, young, premenopausal women from the United Kingdom, France, Belgium, and the United States. J Bone Miner Res. 2009; 24:389–397. [PubMed: 18665786]
20. Bendre MS, Margulies AG, Walser B, Akel NS, Bhattacharrya S, Skinner RA, Swain F, Ramani V, Mohammad KS, Wessner LL, Martinez A, Guise TA, Chirgwin JM, Gaddy D, Suva LJ. Tumor-derived interleukin-8 stimulates osteolysis independent of the receptor activator of nuclear factor-kappaB ligand pathway. Cancer Res. 2005; 65:11001–11009. [PubMed: 16322249]
21. Kelly T, Suva LJ, Huang Y, Macleod V, Miao HQ, Walker RC, Sanderson RD. Expression of Heparanase by Primary Breast Tumors Promotes Bone Resorption in the Absence of Detectable Bone Metastases. Cancer Res. 2005; 65:5778–5784. [PubMed: 15994953]
22. Ben-Baruch A, Bengali KM, Biragyn A, Johnston JJ, Wang JM, Kim J, Chuntharapai A, Michiel DF, Oppenheim JJ, Kelvin DJ. Interleukin-8 receptor beta. The role of the carboxyl terminus in signal transduction. J Biol Chem. 1995; 270:9121–9128. [PubMed: 7721826]
23. Ben-Baruch A, Bengali K, Tani K, Xu L, Oppenheim JJ, Wang JM. IL-8 and NAP-2 differ in their capacities to bind and chemoattract 293 cells transfected with either IL-8 receptor type A or type B. Cytokine. 1997; 9:37–45. [PubMed: 9067094]

24. Simonet WS, Hughes TM, Nguyen HQ, Trebasky LD, Danilenko DM, Medlock ES. Long-term impaired neutrophil migration in mice overexpressing human interleukin-8. J Clin Invest. 1994; 94:1310–1319. [PubMed: 7521886]
25. Hanson JC, Bostick MK, Campe CB, Kodali P, Lee G, Yan J, Maher JJ. Transgenic overexpression of interleukin-8 in mouse liver protects against galactosamine/endotoxin toxicity. J Hepatol. 2006; 44:359–367. [PubMed: 16168518]
26. Bouxsein ML, Boyd SK, Christiansen BA, Guldberg RE, Jepsen KJ, Muller R. Guidelines for assessment of bone microstructure in rodents using micro-computed tomography. J Bone Miner Res. 2010; 25:1468–1486. [PubMed: 20533309]
27. Fowler TW, McKelvey KD, Akel NS, Vander Schilden J, Bacon AW, Bracey JW, Sowder T, Skinner RA, Swain FL, Hogue WR, Leblanc DB, Gaddy D, Wenger GR, Suva LJ. Low bone turnover and low BMD in Down syndrome: effect of intermittent PTH treatment. PLoS One. 2012; 7:e42967. [PubMed: 22916188]
28. Suva LJ, Hartman E, Dilley JD, Russell S, Akel NS, Skinner RA, Hogue WR, Budde U, Varughese KI, Kanaji T, Ware J. Platelet dysfunction and a high bone mass phenotype in a murine model of platelet-type von Willebrand disease. Am J Pathol. 2008; 172:430–439. [PubMed: 18187573]
29. Perrien DS, Akel NS, Edwards PK, Carver AA, Bendre MS, Swain FL, Skinner RA, Hogue WR, Nicks KM, Pierson TM, Suva LJ, Gaddy D. Inhibin A is an endocrine stimulator of bone mass and strength. Endocrinology. 2007; 148:1654–1665. [PubMed: 17194739]
30. Washam CL, Byrum SD, Leitzel K, Ali SM, Tackett AJ, Gaddy D, Sundermann SE, Lipton A, Suva LJ. Identification of PTHrP(12–48) as a plasma biomarker associated with breast cancer bone metastasis. Cancer Epidemiol Biomarkers Prev. 2013; 22:972–983. [PubMed: 23462923]
31. Bertini R, Allegretti M, Bizzarri C, Moriconi A, Locati M, Zampella G, Cervellera MN, Di Cioccio V, Cesta MC, Galliera E, Martinez FO, Di Bitondo R, Troiani G, Sabbatini V, D'Anniballe G, Anacardio R, Cutrin JC, Cavalieri B, Mainiero F, Strippoli R, Villa P, Di Girolamo M, Martin F, Gentile M, Santoni A, Corda D, Poli G, Mantovani A, Ghezzi P, Colotta F. Noncompetitive allosteric inhibitors of the inflammatory chemokine receptors CXCR1 and CXCR2: prevention of reperfusion injury. Proc Natl Acad Sci U S A. 2004; 101:11791–11796. [PubMed: 15282370]
32. Salcedo R, Martins-Green M, Gertz B, Oppenheim JJ, Murphy WJ. Combined administration of antibodies to human interleukin 8 and epidermal growth factor receptor results in increased antimetastatic effects on human breast carcinoma xenografts. Clin Cancer Res. 2002; 8:2655–2665. [PubMed: 12171898]
33. Aalinkeel R, Nair MP, Sufrin G, Mahajan SD, Chadha KC, Chawda RP, Schwartz SA. Gene expression of angiogenic factors correlates with metastatic potential of prostate cancer cells. Cancer Res. 2004; 64:5311–5321. [PubMed: 15289337]
34. Zhu YM, Webster SJ, Flower D, Woll PJ. Interleukin-8/CXCL8 is a growth factor for human lung cancer cells. Br J Cancer. 2004; 91:1970–1976. [PubMed: 15545974]
35. Chung HW, Jang S, Lim JB. Clinical implications and diagnostic usefulness of correlation between soluble major histocompatibility complex class I chain-related molecule a and protumorigenic cytokines in pancreatic ductal adenocarcinoma. Cancer. 2013; 119:233–244. [PubMed: 22736451]
36. Ewington L, Taylor A, Sriraksa R, Horimoto Y, Lam EW, El-Bahrawy MA. The expression of interleukin-8 and interleukin-8 receptors in endometrial carcinoma. Cytokine. 2012; 59:417–422. [PubMed: 22626766]
37. Li KC, Huang YH, Ho CY, Chu CY, Cha ST, Tsai HH, Ko JY, Chang CC, Tan CT. The role of IL-8 in the SDF-1alpha/CXCR4-induced angiogenesis of laryngeal and hypopharyngeal squamous cell carcinoma. Oral Oncol. 2012; 48:507–515. [PubMed: 22366438]
38. Zakrzewska I, Kozlowski L, Wojtukiewicz M. Value of interleukin-8 determination in diagnosis of benign and malignant breast tumor. Pol Merkuriusz Lek. 2002; 13:302–304.
39. Lehrer S, Diamond EJ, Mamkine B, Stone NN, Stock RG. Serum interleukin-8 is elevated in men with prostate cancer and bone metastases. Technol Cancer Res Treat. 2004; 3:411. [PubMed: 15453805]
40. St John MA, Li Y, Zhou X, Denny P, Ho CM, Montemagno C, Shi W, Qi F, Wu B, Sinha U, Jordan R, Wolinsky L, Park NH, Liu H, Abemayor E, Wong DT. Interleukin 6 and interleukin 8 as

potential biomarkers for oral cavity and oropharyngeal squamous cell carcinoma. Arch Otolaryngol Head Neck Surg. 2004; 130:929–935. [PubMed: 15313862]

41. Boucharaba A, Serre CM, Gres S, Saulnier-Blache JS, Bordet JC, Guglielmi J, Clezardin P, Peyruchaud O. Platelet-derived lysophosphatidic acid supports the progression of osteolytic bone metastases in breast cancer. J Clin Invest. 2004; 114:1714–1725. [PubMed: 15599396]
42. Korkaya H, Liu S, Wicha MS. Breast cancer stem cells, cytokine networks, and the tumor microenvironment. J Clin Invest. 2011; 121:3804–3809. [PubMed: 21965337]
43. Lin Y, Huang R, Chen L, Li S, Shi Q, Jordan C, Huang RP. Identification of interleukin-8 as estrogen receptor-regulated factor involved in breast cancer invasion and angiogenesis by protein arrays. Int J Cancer. 2004; 109:507–515. [PubMed: 14991571]
44. Moscova M, Marsh DJ, Baxter RC. Protein chip discovery of secreted proteins regulated by the phosphatidylinositol 3-kinase pathway in ovarian cancer cell lines. Cancer Res. 2006; 66:1376–1383. [PubMed: 16452192]
45. Van Damme J, Decock B, Lenaerts JP, Conings R, Bertini R, Mantovani A, Billiau A. Identification by sequence analysis of chemotactic factors for monocytes produced by normal and transformed cells stimulated with virus, double-stranded RNA or cytokine. Eur J Immunol. 1989; 19:2367–2373. [PubMed: 2691259]
46. Van den Steen PE, Proost P, Wuyts A, Van Damme J, Opdenakker G. Neutrophil gelatinase B potentiates interleukin-8 tenfold by aminoterminal processing, whereas it degrades CTAP-III, PF-4, and GRO- alpha and leaves RANTES and MCP-2 intact. Blood. 2000; 96:2673–2681. [PubMed: 11023497]
47. Van Den Steen PE, Wuyts A, Husson SJ, Proost P, Van Damme J, Opdenakker G. Gelatinase B/MMP-9 and neutrophil collagenase/MMP-8 process the chemokines human GCP-2/CXCL6, ENA-78/CXCL5 and mouse GCP-2/LIX and modulate their physiological activities. Eur J Biochem. 2003; 270:3739–3749. [PubMed: 12950257]

## Highlights

- Patient breast tumor IL-8 expression is not correlated with estrogen receptor status
- Breast cancer patient bone resorption is significantly correlated with IL-8 levels
- Tumor-derived and transgenic IL-8 expression drives bone resorption *in vivo* in mice
- Modulation of IL-8 expression controls osteolytic phenotype of breast cancer cells in mice

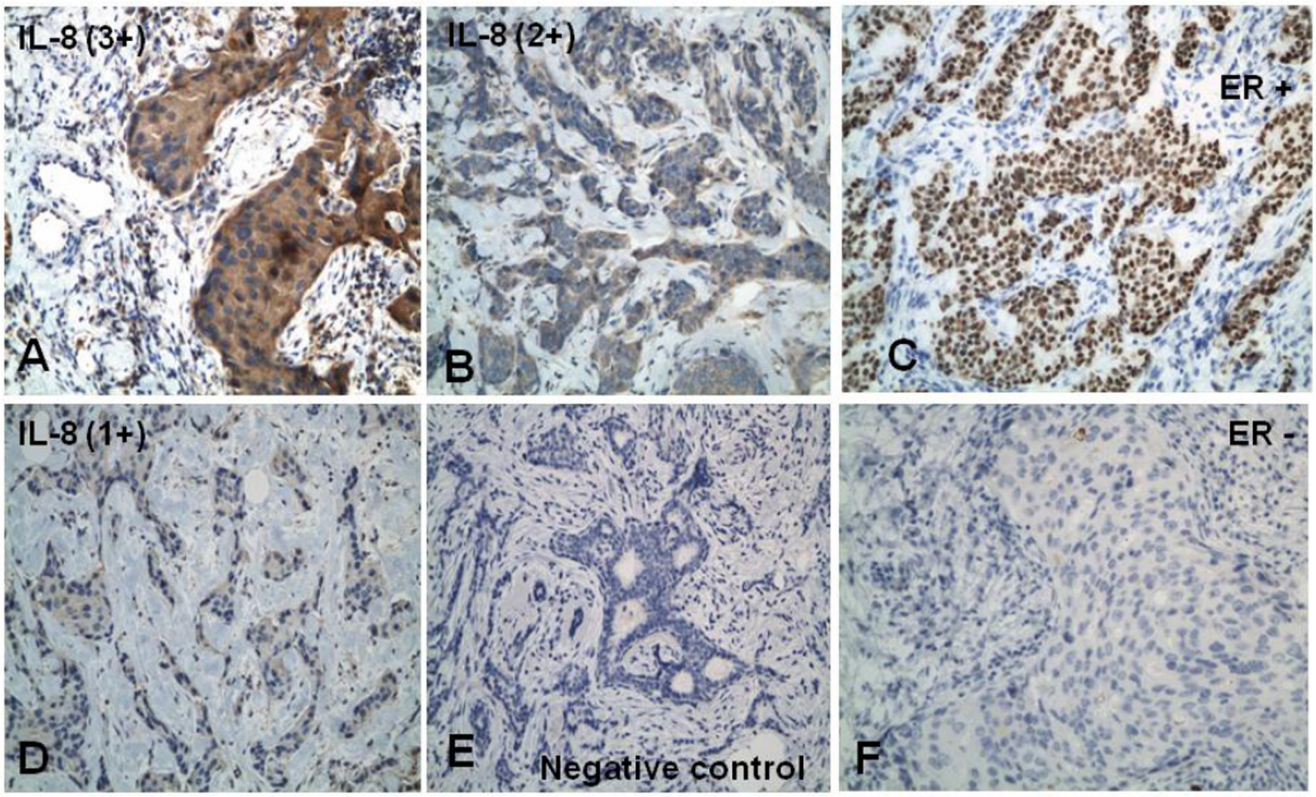


**Figure 1. IL-8 expression is common in primary human breast cancer**

(**A, B, D, E**) 3+, 2+, 1+ intensity, and negative IL-8 staining, respectively, with Horse radish peroxidase visualization (brown stain) and Hematoxylin counter stain. (**C**) ER positive breast cancer case (**F**) ER negative breast cancer case.

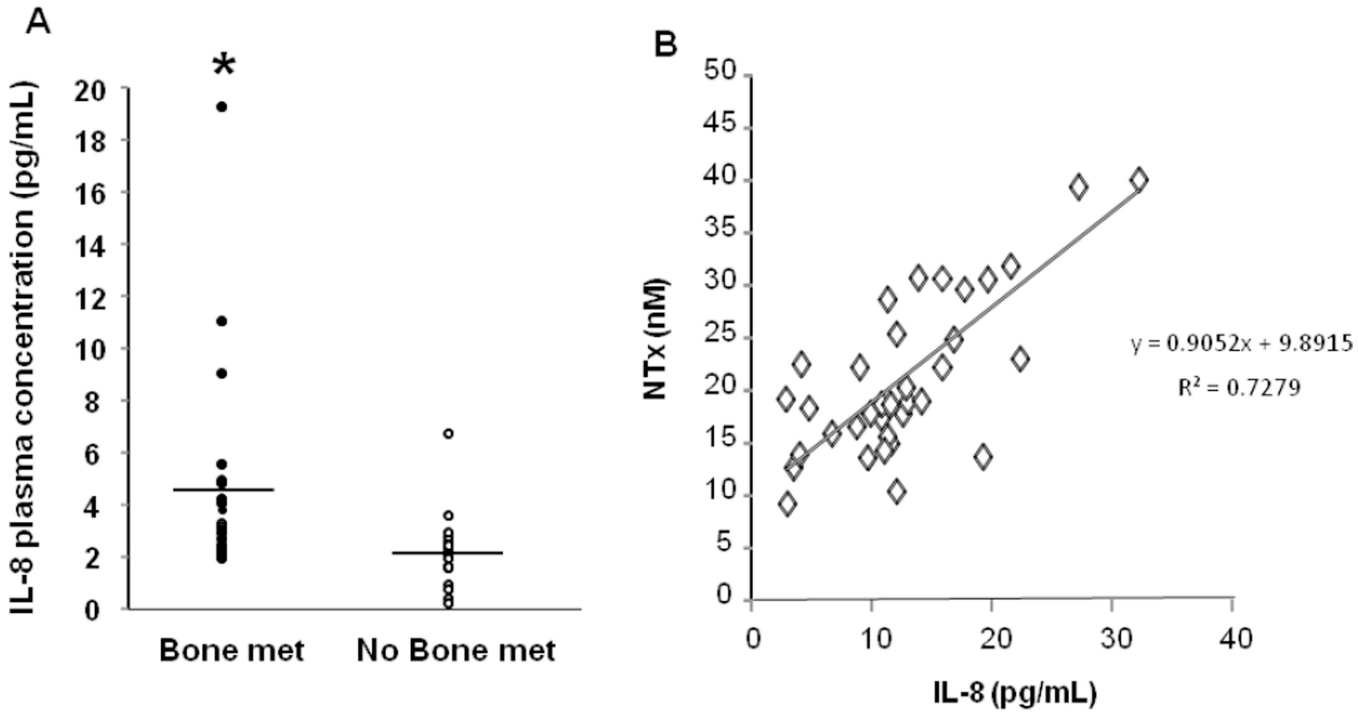


**Figure 2. IL-8 expression is significantly correlated with bone resorption**

(**A**) Plasma IL-8 levels measured in breast cancer patients with and without bone metastasis. Bone metastasis patients IL-8 levels are significantly higher than no bone metastasis patients (* $p<0.05$). (**B**) A significant correlation exists between serum NTx and plasma IL-8 levels ($R^2 = 0.7279$).

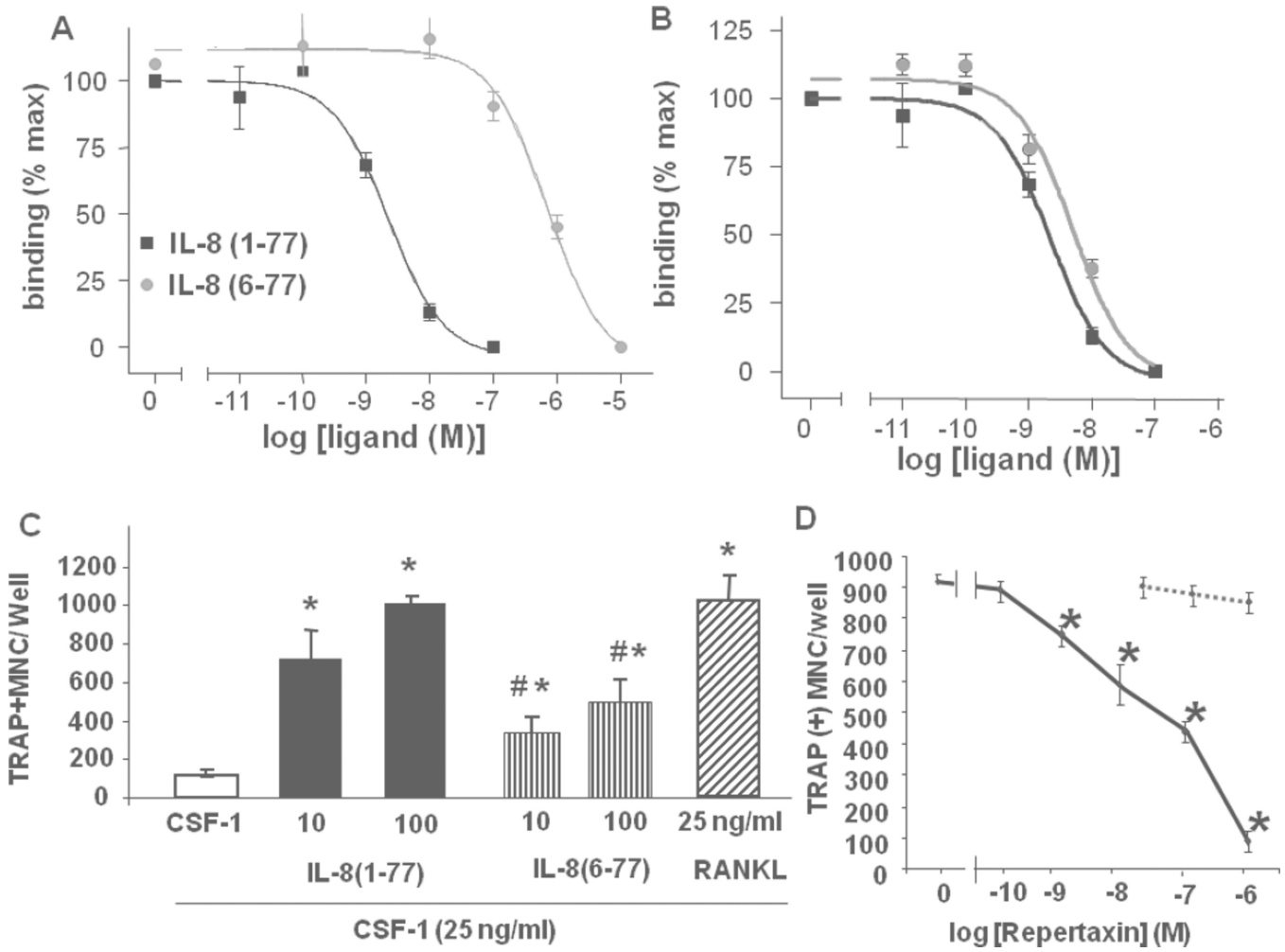


**Figure 3. IL-8 osteoclastogenesis activity correlates with ligand CXCR1 affinity**

Specific binding of IL-8(1–77) (squares) and IL-8(6–77) (circles) to HEK-293 cells expressing CXCR1 (**A**) or CXCR2 (**B**). (**C**) TRAP positive multinucleated cell formation in the presence of CSF-1 (25 ng/ml) and either IL-8(1–77) (10, 100 ng/mL; black bars), IL-8(6–77) (10, 100 ng/mL; vertical striped bars) or RANKL (25 ng/mL; slashed bar). * significantly different from CSF-1 (control) ($p<0.05$); # significantly different from IL-8(1–77). ($p<0.05$). (**D**) Dose-dependent inhibition of IL-8(1–77) stimulated TRAP positive multinucleated cell formation by Repertaxin (solid line). No effect of Repertaxin on RANKL-stimulated TRAP positive multinucleated cell formation (dashed line). * $p<0.05$. Results are typical of three independent experiments.

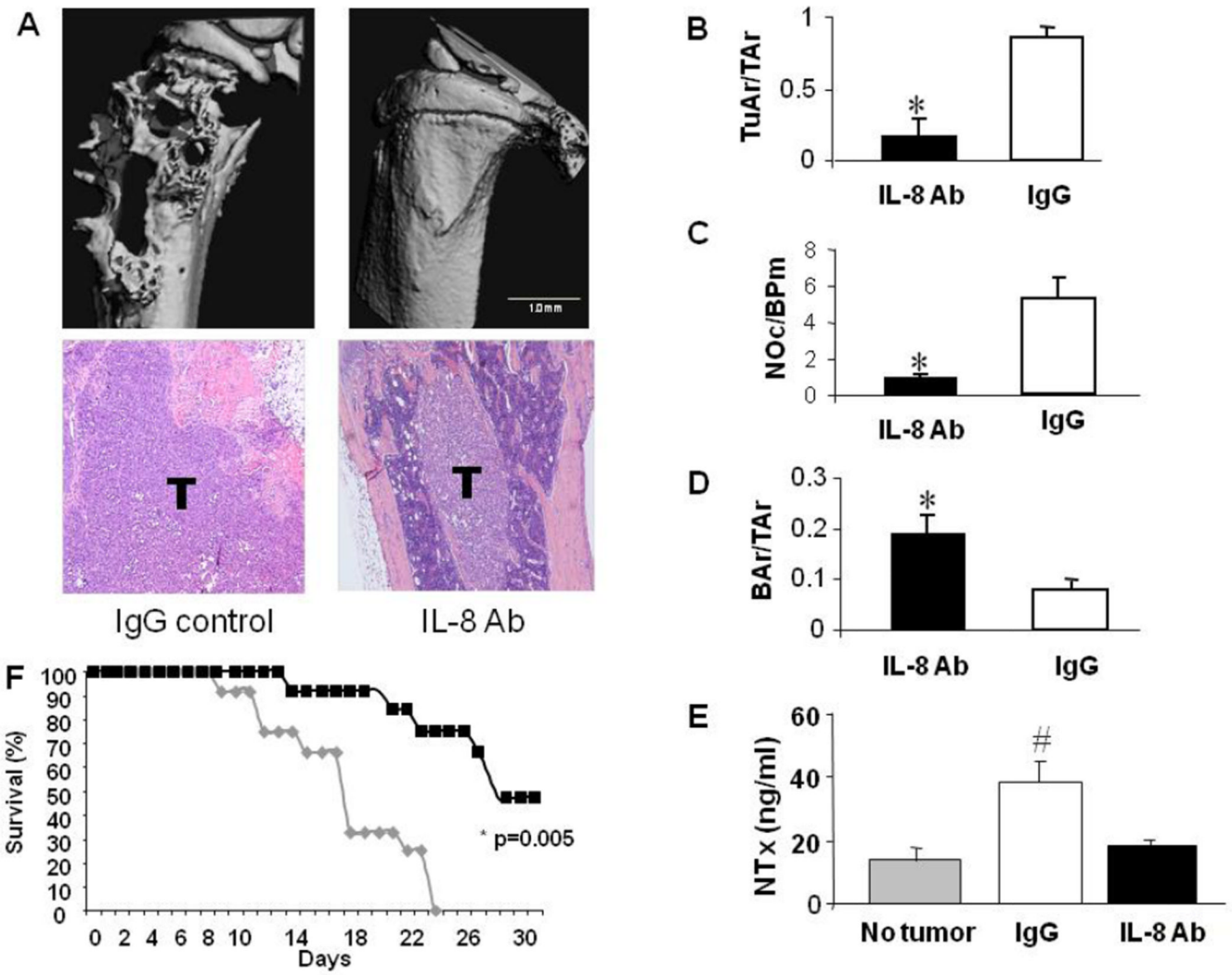


**Figure 4. Anti-IL-8 antibody treatment significantly alters tumor progression in bone**

(**A**) MicroCT renderings and H&E histology (10× magnification) of IgG control (20 mice) and IL-8 antibody (IL-8 Ab; 20 mice) treated MDA-MET tumor bearing nude mice (females inoculated at 4 weeks of age). Severe osteolysis and rampant tumor growth is observed in IgG treated animals (T) compared with IL-8 Ab treated animals. (**B–D**) Histomorphometric evaluation of tumor area/total area (TuAr/TAr), number of osteoclasts/bone perimeter (NOc/BPm) and bone area/total area (BAr/TAr) for IL8 Ab treated (black bars) and IgG treated (white bars) animals. * significantly different from IgG treatment $p<0.05$. (**E**) Serum NTx levels in non tumor-bearing controls (gray bar), and IgG (white bar) and IL-8 Ab (black bar) treated tumor bearing mice. # significantly different from no tumor control $p<0.05$ (**F**) Kaplan Meier plot showing significant improvement in survival with IL-8 antibody treatment. The IL-8 antibody treated group (30 mice) (black squares) showed a significant increase in survival compared with the IgG group (30 mice) (gray diamonds) ($P = 0.005$). IC50 for survival was 17 days for IgG treated and 28 days for IL-8 antibody treated groups.

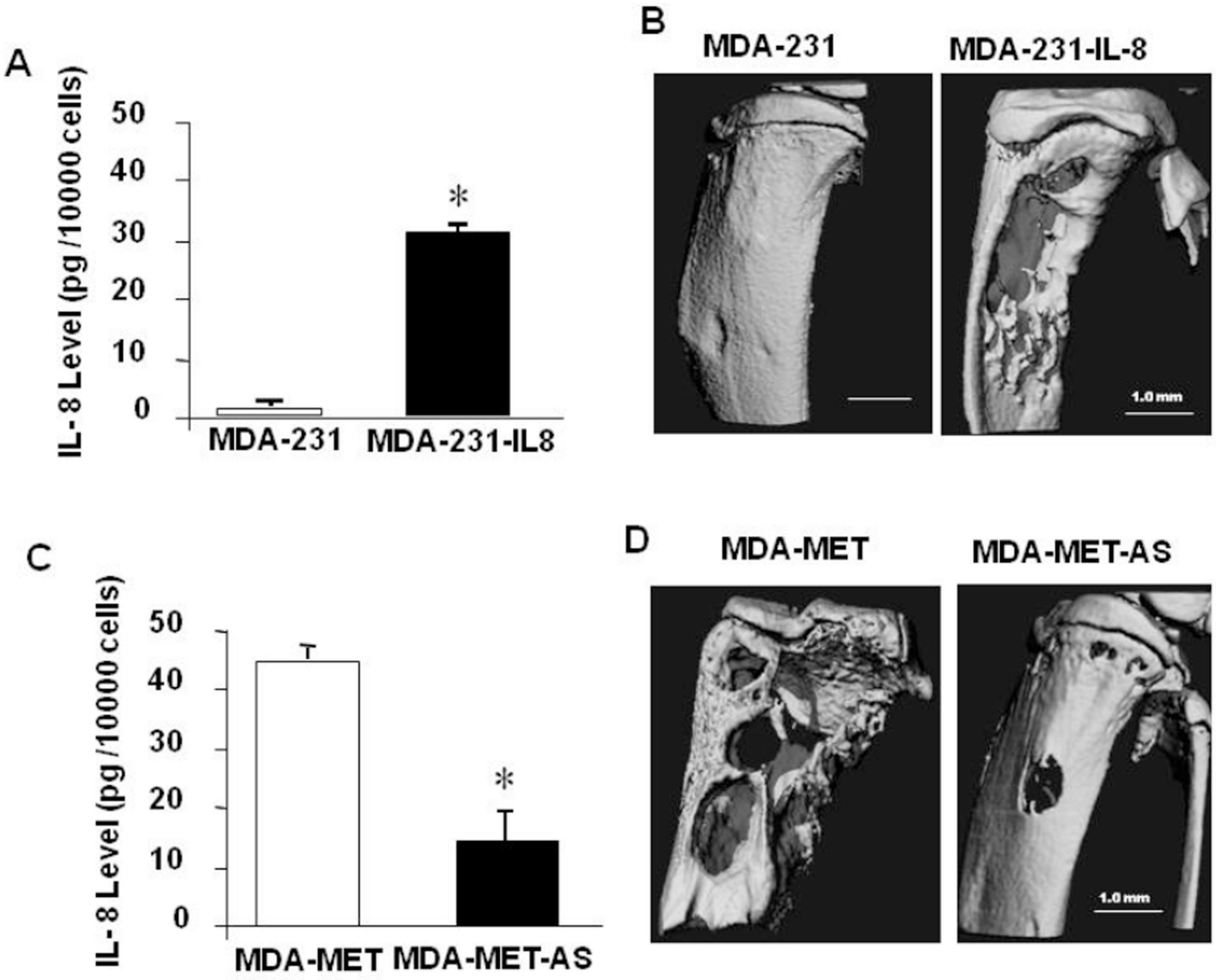


**Figure 5. IL-8 expression regulates tumor growth in bone**

**(A)** IL-8 expression in conditioned medium from MDA-231 and MDA-231-IL8 cells. IL-8 levels are significantly higher in MDA-231-IL8 cells. * $p<0.05$. (**B**) MicroCT renderings of MDA-231 and MDA-231-IL8 tumor bearing nude mouse tibia (10 females/group inoculated with tumor at 4 weeks of age). (**C**) IL-8 expression in conditioned medium MDA-MET and MDA-MET-AS cells. IL-8 levels are significantly lower in MDA-MET-AS cells. * $p<0.05$. (**D**) MicroCT renderings of MDA-MET and MDA-MET-AS tumor bearing nude mouse tibia (10 females/group inoculated with tumor at 4 weeks of age).

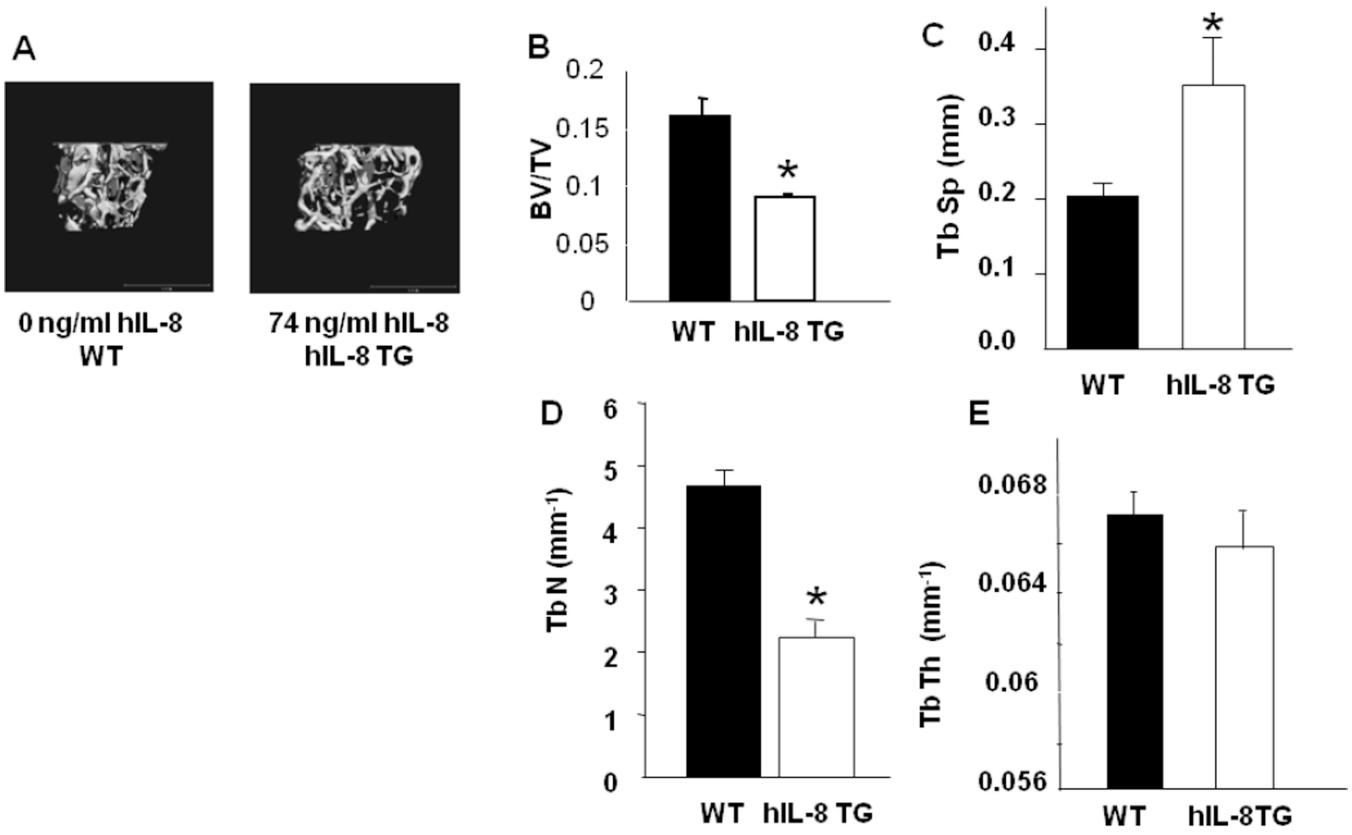


**Figure 6. IL-8 transgenic mice have low bone mass phenotype**

(**A**) MicroCT renderings of trabecular bone of the proximal tibia of WT and human IL-8 transgenic (hIL-8 TG) mice. Specific levels of human IL-8 for these specific animals are shown. (**B–E**) MicroCT measured parameters of trabecular microarchitecture in WT and hIL-8 TG mice. BV/TV (bone volume/total volume); TbSp (trabecular spacing); TbN (trabecular number); TbTh (trabecular thickness). * significantly different from WT. $p<0.05$.

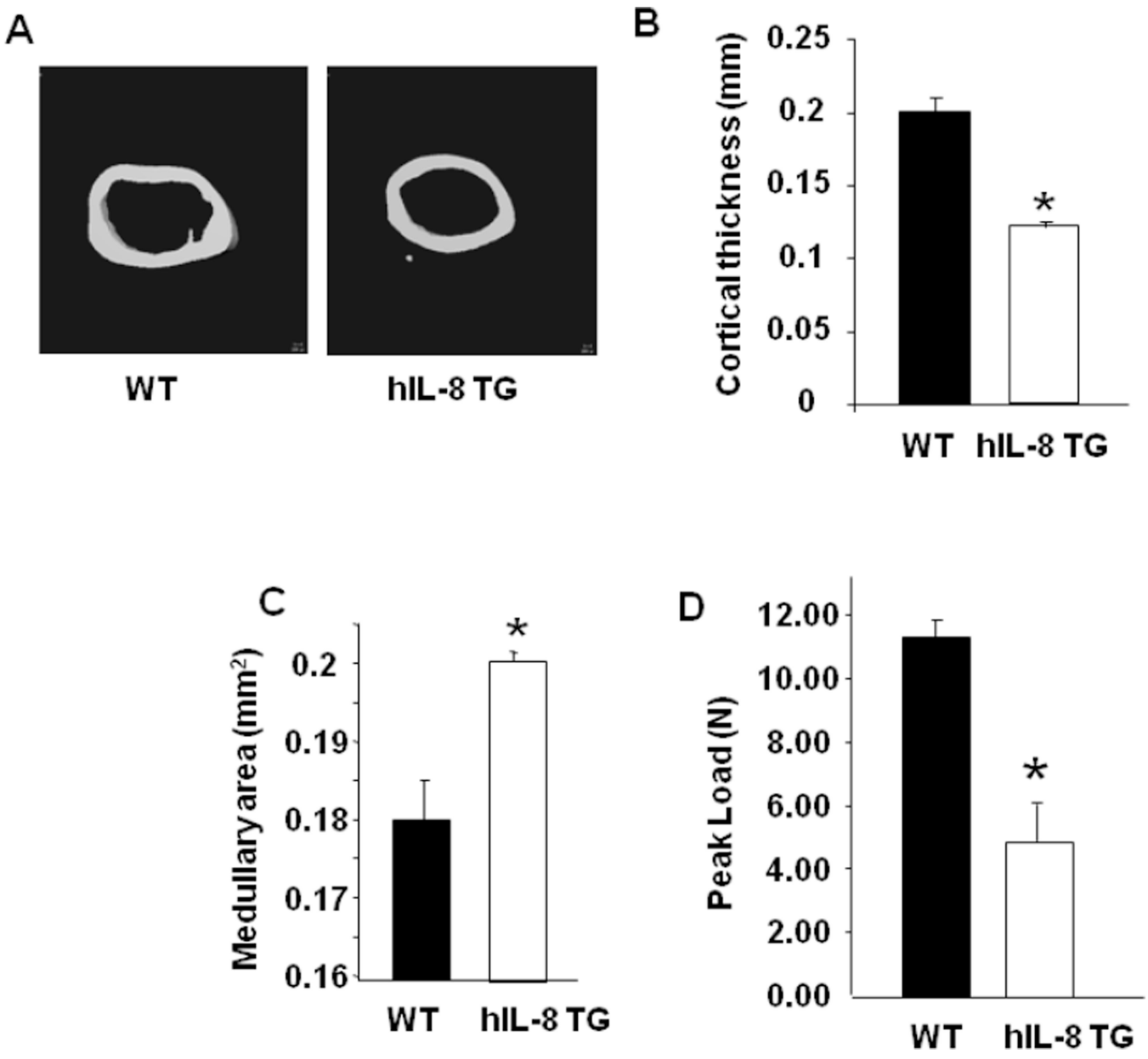


**Figure 7. Cortical bone phenotype of IL-8 transgenic mice**

(**A**) MicroCT renderings of 25 consecutive 9 μm slices of cortical bone of the femur mid-shaft of WT and human IL-8 transgenic (hIL-8 TG) mice. (**B, C**) MicroCT measured parameters of cortical geometry in WT and hIL-8 TG mice. Cortical Thickness and Medullary Area, respectively. (**D**) Peak load to failure for WT and hIL-8 TG mice femurs. * significantly different from WT. $p<0.05$.

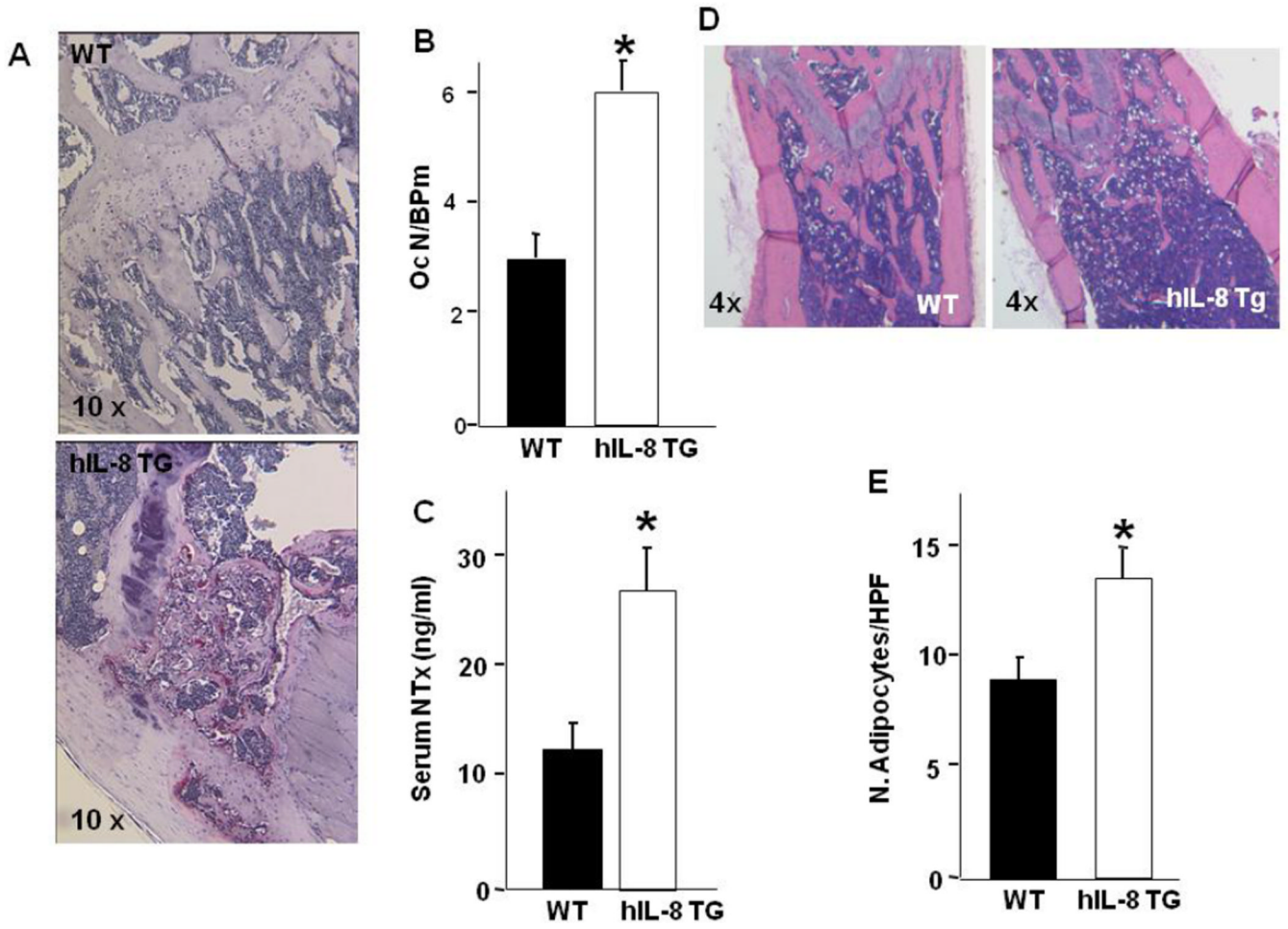


**Figure 8. Transgenic IL-8 expression *in vivo* increases osteoclast formation and adipogenesis**

(**A**) TRAP stained H&E histology (10× magnification) of WT and hIL-8 TG mice. Red staining shows TRAP-positive osteoclasts *in vivo*. (**B**) Quantitation of osteoclast number/bone perimeter (NOc/BPm) for WT and hIL-8 TG mice. * significantly different from WT. $p<0.05$. (**C**) Serum IL-8 levels (mean ± SEM) measured in WT (n=6) and hIL-8 TG mice (n=7). * significantly different from WT. $p<0.05$. (**D**) H&E histology (4× magnification) of WT and hIL-8 TG mice. Numerous white adipocyte ghosts are apparent in the bone marrow. (**E**) Quantitation of adipocyte number/high powered (20×) field (N. Adipocytes/HPF) for WT and hIL-8 TG mice. * significantly different from WT. $p<0.05$.

## Table 1

| ER Status | Total cases | IL-8 Expression | | |
|---|---|---|---|---|
| | | 3+ | 2+ | 1+ |
| ER + | 22 | 15 (68%) | 6 (27%) | 1 (5%) |
| ER − | 15 | 7 (47%) | 7 (47%) | 1 (6%) |

Invasive ductal carcinomas of the breast express IL-8. IL-8 expression *in vivo* does not correlate with ER status, contrary to previously published in vitro observations.